

Evidence of dark energy in different cosmological observations

Arindam Mazumdar^{1,a}, Subhendra Mohanty^{2,b}, and Priyank Parashari^{2,3,c}

¹ Department of Physics, Indian Institute of Technology Kharagpur, India - 721302

² Theoretical Physics Division, Physical Research Laboratory, Navrangpura, Ahmedabad - 380009, India.

³ Indian Institute of Technology, Gandhinagar, 382355, India

Abstract. The idea of a negative pressure dark energy component in the Universe which causes an accelerated expansion in the late Universe has deep implications in models of field theory and general relativity. In this article, we survey the evidence for dark energy from cosmological observations which started from the compilation of distance-luminosity plots of Type Ia supernovae. This turned out to be consistent with the dark energy inferred from the CMB observations and large scale surveys and gave rise to the concordance Λ CDM model of cosmology. In this article, we discuss the observational evidence for dark energy from Type Ia supernovae, CMB, galaxy surveys, observations of the Sunyaev-Zeldovich effect from clusters, and lensing by clusters. We also discuss the observational discrepancy in the values of H_0 and σ_8 between CMB and large scale structures and discuss if varying dark energy models are able to resolve these tensions between different observations.

1 Introduction

The idea of a cosmological constant was introduced by Einstein to counteract the expansion in the Universe caused by normal matter as 'Einstein's Universe' was designed to be static. Later the concept of the cosmological constant evolved to the idea that it was a form of vacuum energy with positive energy density and negative pressure whose effect at cosmological scales would be to cause an accelerated expansion of the Universe. The idea of vacuum energy has been known since the prediction and observation of the 'Casimir effect' which arises from the virtual electron-positron pairs produced from the vacuum. From the point of quantum field theory, the existence of the cosmological vacuum energy would be natural, however, the problem is that the scale of vacuum energy expected in particle physics would be many orders of magnitude different from the energy density of the Universe, and this problem is usually called the 'cosmological constant problem' [1]. Another problem from the purely cosmological perspective is to explain why the cosmological constant which does not change with the expansion of the Universe happens to be of the same order

^a e-mail: arindam.mazumdar@iitkgp.ac.in

^b e-mail: mohanty@prl.res.in

^c e-mail: parashari@prl.res.in

of magnitude as the matter in the present Universe since the two vary differently during the expansion history of the Universe. This ‘why now’ problem is explained by coupling dark matter to normal matter so that they track each other over the cosmological history of the Universe.

From the observational perspective, the first confirmation of an accelerated expanding Universe came from the measurement of luminosity distance plots of Type Ia supernovae by Riess et. al [2] and Perlmutter et al. [3], which prompted the rebirth of the idea of a dark energy dominated Universe in the present epoch. Subsequently, the observations of CMB anisotropy and large scale structures confirmed the evidence of an accelerating phase for the low redshift Universe. The observations of supernovae luminosity, CMB and large scale structures give a concordance model called Λ CDM cosmology where the present Universe comprises about 68% dark energy, 27% dark matter and 5% baryonic matter. However not all is well with the Λ CDM model, for example, there is a $4\text{-}\sigma$ discrepancy between the observation of the Hubble expansion rate at present epoch (H_0) derived from the CMB and those from the local measurements. These discrepancies may be addressed by the evolving dark energy models.

In this article, we will very briefly review the different ways of measuring dark energy parameters and the current status of individual measurements as well as joint analyses.

The Hubble parameter which determines the rate of the expansion in an FLRW Universe depends on different components of the Universe in the following way

$$H(z) = H_0 \sqrt{\Omega_m(1+z)^3 + \Omega_{\text{DE}}f(z) + \Omega_k(1+z)^2 + \Omega_r(1+z)^4}, \quad (1)$$

where z represents the redshift, Ω_m is the matter density fraction, Ω_r is the radiation density fraction, Ω_k is the energy density fraction corresponds to spatial curvature of the FLRW metric and Ω_{DE} is the energy density fraction of dark energy at present with

$$f(z) = \exp \left[3 \int_0^z \frac{1+w(z')}{1+z'} dz' \right]. \quad (2)$$

Here $w(z)$ defines the equation of state the dark energy. We will consider three different types of dark energy scenarios; namely, the cosmological constant when $\Omega_{\text{DE}} = \Omega_\Lambda$ and $w(z) = -1$; dark energy with a fixed non-zero equation of state parameter when $w(z) = w$ (known as w CDM model); and dark energy with varying equation of state parameter. For the last case, we consider the equation of state of dark energy to be characterized by the CPL parameterization [4,5]

$$w(a) = w_0 + w_a(1-a), \quad (3)$$

where a is the scale factor of the FLRW metric of the Universe.

For all the above-mentioned cases we will study the recent observational status from different ways of measuring dark energy. So far there are three different ways to measure the dark energy. The first one is through the measuring the expansion rate of the Universe directly from the standard candles (type Ia supernovae). After the discovery of gravitational waves in LIGO, the chirping frequency of the gravity wave from the binary mergers, which acts as a standard siren, has opened up a new window of measuring the distance of the binary system. If the binary system emits any electro-magnetic signal at the time of the merger, the redshift of the signal can provide information about the velocity of the combined system. This can help to infer the expansion rate of the Universe directly. However, this method would require the next few decades of observation to constrain dark energy parameters efficiently.

The second type of the measurement is using the Baryon Acoustic Oscillation (BAO) scale as the standard ruler. This type of measurement provides the integrated history of $H(z)$ evolution. The third type of observations measures the growth rate of the dark matter density perturbations at late time. These types of observations are the large scale structure surveys like lensing surveys, Sunyaev-Zeldovich (SZ) surveys, galaxy surveys and, in future, the 21-cm surveys.

We organise the article in the following way. In section 2,3 and 4 we describe the above mentioned three different methods of determining dark energy parameters. In these sections we presented the recent results of the observations in tabulated format (table 1 and 2). Then in two small sections, section 5 and section 6 we discuss the current issues in reconstructing dark energy equation of state from the observations and various attempts to resolve the H_0 tension by modifying the dark energy sector. Then we summarise the current status of all the observations in section 8.

2 Measurement from the observations of type Ia supernovae

In a binary system, the mass of a white dwarf increases either due to accretion from the other star or due to merger. A type Ia supernovae (SNIa) occur when a white dwarf in a binary system explodes as its mass reaches the Chandrasekhar limit. These supernovae are the brightest of all the supernovae and they follow quite a similar light curve with a consistent peak luminosity. That is why we can use these supernovae as the standard candles to measure the distances. However, there are a few difficulties and problems with SNIa observations. For example, after the supernovae explosion, SNIa reaches the peak luminosity in a few weeks after that these SNIa fade away within a few months. Also, it is very difficult to predict a supernovae explosion event and these events take place a few times per millennium in a galaxy. Therefore, this makes it very difficult to track all the events. In addition, although most SNIa has quite a similar light curve, a few SNIa is either a little bit fainter or brighter [6]. Moreover, the SNIa are observed in a particular band filter depending on their peak luminosity. However, some part of the spectrum, other than the observing filter, comes from the filter during observations. Therefore, we need to correct this difference in the spectrum to get the accurate results [6]. Finally, the distance modulus from the observation (μ_{obs}) of SNIa can be obtained as [7,8]

$$\mu_{\text{obs}} = m_B + \alpha x_1 - \beta C + M_0 + \gamma G_{\text{host}} + \Delta\mu_{\text{bias}}, \quad (4)$$

where M_0 is the absolute magnitude of SNIa and $m_B = -2.5 \log(x_0)$ with x_0 being the amplitude of the light curve. Here, x_1 and C represent the light curve width and color for each SNIa, respectively. Moreover, α characterize the relation between SNIa luminosity and width of SNIa light curve, and β describes the correlation between color and SNIa luminosity. These parameters are obtained by fitting the light curve for each SNIa. Furthermore, γ accounts for the correction due to host-galaxy stellar mass and $G_{\text{host}} = +1/2$ if host-galaxy stellar mass is larger than 10^{10} solar mass, and $G_{\text{host}} = -1/2$ if host-galaxy stellar mass is smaller than 10^{10} solar mass. At last, $\Delta\mu_{\text{bias}}$ is determined from simulation and accounts for the selection bias.

Cosmology with supernovae depends on the luminosity distance measurement as a function of redshift for a number of SNIa and comparing the observed results with the theoretical prediction of distances in different cosmological models. Given a cosmological model, luminosity distance $d_L(z)$ to a source at redshift z can be calculated

Experiment	Model	Ω_A	w	w_0	w_a
Pantheon-SN-stat	Λ CDM	0.716 ± 0.012	-	-	-
Pantheon-SN-stat	w CDM	-	-1.251 ± 0.144	-	-
Pantheon-SN	Λ CDM	0.702 ± 0.022	-	-	-
Pantheon-SN	w CDM	-	-1.090 ± 0.220	-	-
Pantheon-SN+CMB	w CDM	-	-1.026 ± 0.041	-	-
Pantheon-SN+CMB	$w_0 w_a$ CDM	-	-	-1.009 ± 0.159	-0.129 ± 0.755
Pantheon-SN+CMB+BAO	w CDM	-	-1.014 ± 0.040	-	-
Pantheon-SN+CMB+BAO	$w_0 w_a$ CDM	-	-	-993 ± 0.087	-0.126 ± 0.384
DES-SN3YR	Λ CDM	0.669 ± 0.038	-	-	-
DES-SN3YR+CMB	Λ CDM	0.670 ± 0.032	-	-	-
DES-SN3YR+CMB	w CDM	-	-0.978 ± 0.059	-	-
DES-SN3YR+CMB+BAO	Λ CDM	0.690 ± 0.008	-	-	-
DES-SN3YR+CMB+BAO	w CDM	-	-0.977 ± 0.047	-	-
DES-SN3YR+CMB+BAO	$w_0 w_a$ CDM	-	-	-0.885 ± 0.114	-0.387 ± 0.430

Table 1. The values of dark energy related quantities from the SNIa data by pantheon [7] and DES-SN3YR [8] samples and from the combinations of SNIa, CMB [9] and BAO [10,11,12,13] data are shown in this table.

by the following relation

$$d_L(z) = \frac{c}{H_0} (1+z) \times \begin{cases} \frac{1}{\sqrt{|\Omega_k|}} \sinh(\sqrt{|\Omega_k|} \int_0^z \frac{dz'}{E(z')}) & \Omega_k > 0 \\ \int_0^z \frac{dz'}{E(z')} & \Omega_k = 0 \\ \frac{1}{\sqrt{|\Omega_k|}} \sin(\sqrt{|\Omega_k|} \int_0^z \frac{dz'}{E(z')}) & \Omega_k < 0 \end{cases} \quad (5)$$

where $E(z) = \frac{H(z)}{H_0}$ and $H(z)$ is given by eq. (1) and c is the speed of light. Once we know the luminosity distance, we can calculate the distance modulus (μ_{th}) for a given theoretical model as

$$\mu_{th} = 5 \log_{10}(d_L(z)/10pc). \quad (6)$$

Now, after comparing the theoretical and observational predictions for the distance modulus, we can put constraints on the cosmological parameters.

In 1998, it was first discovered by Riess et. al [2] using the SNIa data from Hubble space telescope (HST) observation that the Universe is expanding at an accelerating rate. In 1999, using the data of 42 SNIa, Perlmutter et al. [3] had also found that the expansion rate of the Universe is accelerating. Since then the use of SNIa as standard candles has been of critical importance and has attracted great attention in cosmology. Over the last two decades, there have been a number of supernovae surveys by different groups which probed a large redshift range. There have been many surveys which search for SNIa in the low redshift range ($0.01 < z < 0.1$) e.g CfA1-CfA4 [14,15,16,17,18], the Carnegie Supernova Project (CSP) [19,20,21] and the Lick Observatory Supernova Search (LOSS) [22] etc. Moreover, some surveys like the ESSENCE supernova survey [23,24,25], SuperNova Legacy Survey (SNLS) [26,27], Sloan Digital Sky Survey (SDSS) [28,29,30] and Pan-STARRS survey (PS1) [31,32] have assembled SNIa data in the redshift range $z > 0.1$. There are also some other surveys like SCP [33], GOODS [34,35] and CANDELS/CLASH [36,37,38] survey which look for SNIa in high- z range ($z > 1.0$). Data from these surveys had been used to constrain the cosmological parameters. Recently, Scolnic et al. [7] have assembled the data of 1042 SNIa in the redshift range from $z \sim 0.01$ to $z \sim 2.0$ from PS1, CfA1-A4, CSP, SDSS, SNLS, SCP, GOODS and CANDELS/CLASH surveys and called it pantheon sample. They did analysis for different cosmological models with just pantheon-SN data and with the combination of pantheon-SN data and data from other cosmological probes such as CMB and BAO. The results for different cosmological models are shown in table 1. In addition to these, recently Dark Energy

Survey Supernova Program (DES-SN) have also reported 207 SNIa in the redshift range $0.015 < z < 0.7$ [8]. They did the analysis with a total of 329 SNIa in which they have included 122 low redshift SNIa from the literature and called this sample DES-SN3YR. The results for different cosmological models with DES-SN3YR data and data from other probes are also shown in table 1.

Recently the authors of ref [39] have argued that the cosmic acceleration inferred from the Type Ia supernovae (more particularly the JLA data) has a scale-dependent dipolar modulation. This effect can be attributed to the bulk flow in the local Universe in which the observer is located. Therefore, the direct “evidence” of dark energy can be an artifact of the inhomogeneous nature of the Universe at present time.

3 Measurement from the imprints of baryon acoustic oscillation

The primordial perturbations reenter the horizon at the time of radiation dominated and the matter-dominated era. The photon-baryon fluid in which baryon and photon are strongly coupled by the Thompson scattering undergoes the acoustic oscillations due to the primordial density perturbations encountered during the expansion of the Universe. These acoustic waves set the pattern in the CMB and the galaxy distributions of the Universe. The characteristic length scale of these oscillation patterns, known as the baryon acoustic oscillation (BAO) scale, works as the standard ruler in the Universe in measuring the Hubble parameter and its evolution. It is because the length scale of BAO at the redshift of recombination can be expressed as [40,41]

$$r_s = \int_{z_{\text{rec}}}^{\infty} \frac{c_s}{H(z)} dz = \frac{1}{\sqrt{\Omega_m H_0^2}} \frac{2c}{\sqrt{3z_{\text{eq}} R_{\text{eq}}}} \ln \left[\frac{\sqrt{1 + R_{\text{rec}}} + \sqrt{R_{\text{eq}} + R_{\text{rec}}}}{1 + \sqrt{R_{\text{rec}}}} \right], \quad (7)$$

where R_{rec} and R_{eq} are baryon-photon ratio ($3\rho_b/4\rho_\gamma$) at the time of recombination and radiation matter equality, respectively. Here, c_s is the sound speed in baryon-photon fluid, z_{rec} and z_{eq} are the redshift corresponding to the recombination and radiation matter equality epoch. This r_s can be estimated accurately if the redshift at recombination and the baryon density of the Universe is known properly. Therefore this scale serves the purpose of the standard ruler in estimating the size of the BAO patterns in CMB. Similarly, for the galaxy surveys, the BAO scale is measured at z_{drag} which is the value of redshift when baryons and photons decouple dynamically.

3.1 CMB

Planck measurement of CMB provides the most accurate measurement of the baryon acoustic oscillation peaks. The CMB power-spectrum is calculated using the first order cosmological perturbation theory where the interaction between the baryon and photon are accounted for (see the equations in ref [43]). The Δ_ℓ , which are the Legendre coefficients of the temperature fluctuations in CMB is calculated by solving these Boltzmann equations. The solution of Δ_ℓ has an oscillatory part as well as a damping part. Further, the Δ_ℓ 's are decomposed in terms of spherical harmonics and the two-point correlation between the coefficients of spherical harmonics, which are written as C_ℓ , are calculated. The oscillatory part in C_ℓ corresponds to the BAO and the damping is known as the Silk damping which arises from the viscosity in photon-baryon fluid (see Fig. 1). The oscillatory part of the CMB can be approximated as $\cos(kr_s + \phi)$ where r_s is defined in eq. (7), ϕ is the phase factor which can depend

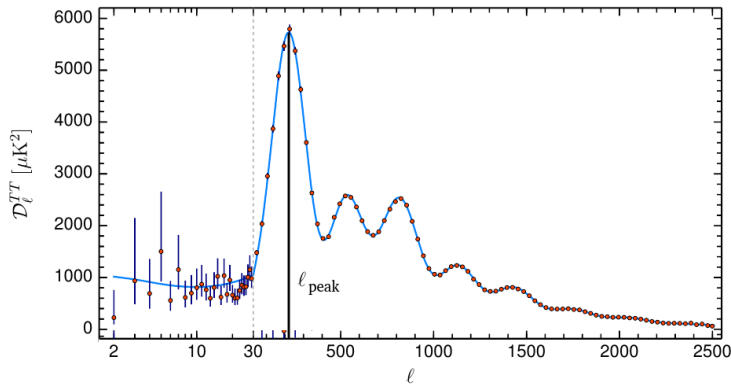


Fig. 1. The figure is taken from Planck-2018 paper [42]. Here $\mathcal{D}_\ell = \ell(\ell + 1)C_\ell/(2\pi)$.

on the effects of the other components of the Universe (dark matter, neutrinos) on CMB. The peak multipoles shown in Fig. 1 is related to the k as

$$\ell_{\text{peak}} = (m\pi - \phi) \frac{D_A}{r_s} = \frac{(m\pi - \phi)}{\theta_*} \quad (8)$$

where, D_A is the angular diameter distance which is given by

$$D_A = \frac{1}{(1 + z_{\text{rec}})} \int_0^{z_{\text{rec}}} \frac{cdz}{H(z)}. \quad (9)$$

The quantity $\theta_* = r_s/D_A$ is known as the angular size of BAO. Planck can measure seven BAO peaks in their CMB pattern and determines the θ_* with an 0.1% accuracy. The information about dark energy, or background cosmology at late time in general, is inferred from CMB through this angular diameter distance. Whereas the Planck CMB data is extremely accurate in predicting the values of Ω_Λ and w of w CDM model, the parameters of varying dark energy show high degeneracy with Planck data alone. To break the degeneracy, complementary observations like BAO and redshift space distortions are also taken into account. The results corresponding to these analyses are shown in table 2.

Apart from the space based surveys like WMAP or Planck, there are some ground based surveys like SPT and ACT survey which also measures the CMB temperature fluctuations in a particular portion of the sky. These experiments can also observe the BAO scales in the CMB and provide the value of the Hubble parameter. For example, the latest value of H_0 inferred from the ACT data alone is 67.9 ± 1.5 km/sec/Mpc $^{-1}$ and Ω_Λ is equal to 0.696 ± 0.022 [44], which are in good agreement with the Planck measurement. It has been reported that SPT data alone provides the value of H_0 to be 73.5 ± 5.2 km/sec/Mpc $^{-1}$ and Ω_Λ is equal to 0.726 ± 0.028 with varying number of relativistic degrees of freedom (N_{eff}) [45].

3.2 Galaxy surveys

The galaxy surveys estimate the values of the position of the galaxies in redshift space from which the galaxy distribution in real space is calculated. The power spectrum of the galaxy field is

$$P_g(k) = b_1^2 P(k), \quad (10)$$

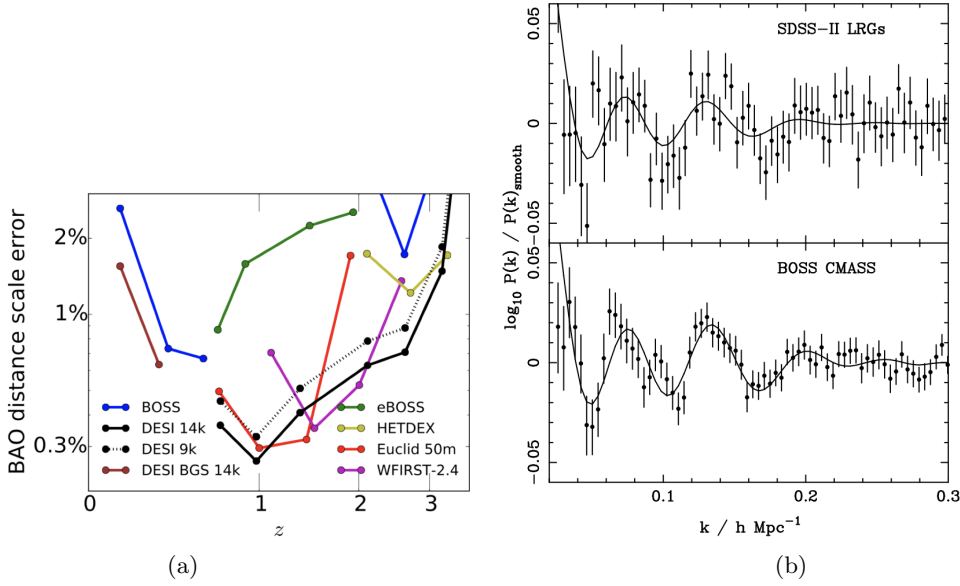


Fig. 2. (a) Accuracy of measurement of BAO scale increased over time with different observation mission. (figure is taken from the site of DESI) (b) Signature of BAO on matter power spectrum. (figure is taken from ref [46])

where b_1 is the linear bias factor and $P(k)$ is the cold dark matter power spectrum. In Fig. 3.2-(b) the matter power spectrum of the observed galaxy field is plotted after subtracting the smooth theoretical power spectrum from it. The left-over power spectrum shows the oscillation pattern of BAO.

From these BAO patterns, the galaxy surveys measure

$$d_z = \frac{r_s(z_{\text{drag}})}{D_V(z)}, \quad (11)$$

where,

$$D_V(z) = \left[(1+z)^2 D_A(z)^2 \frac{cz}{H(z)} \right]^{1/3}. \quad (12)$$

Here, $D_A(z)$, the angular-diameter-distance whose expression is given in eq. (9) in which z_{rec} has to be substituted by the redshift of the galaxies.

The experiments that measure BAO in galaxy power-spectrum are 2dF Galaxy survey [47], SDSS and BOSS [46,48,46,13], Wiggle-Z [49], 6dF galaxy survey [10]. The upcoming galaxy surveys are Euclid [50] and DESI [51]. These galaxy surveys not only provide the BAO pattern but also provides the information of growth factor from redshift space distortion which we will be discussing later in this article.

4 Measurement from the growth rate of large scale structures

The growth rate of density perturbations of cold dark matter in the late time of the evolution of the Universe provides a robust probe to the existence of dark energy and

Experiment	Ω_Λ	w	w_0	w_a
Planck (TT,TE,EE, lowE)	0.6847 ± 0.0073	-	-	-
Planck+SNE+BAO	-	-1.028 ± 0.031	-0.957 ± 0.080	$-0.29^{+0.32}_{-0.26}$
Planck+BAO/RSD+WL	-	-	-0.76 ± 0.20	$-0.72^{+0.62}_{-0.54}$
Planck+JLA+WiggleZ +CFHTLens+SDSS- DR12 [52]	-	-	-0.96 ± 0.10	-0.12 ± 0.32
Planck+SDSS-DR12 [52]	-	-	-1.2 ± 0.32	-0.33 ± 0.75
Planck-SZ + BAO	-	-1.01 ± 0.18	-	-
CFHTLens+WMAP7 +BOSS+HST [53] (for flat Universe)	0.729 ± 0.010	-1.02 ± 0.09	-	-
DES Y1	$0.733^{+0.030}_{-0.017}$	0.82	-	-
DES+Planck+BAO+ SNe	0.702 ± 0.007	$-1^{+0.05}_{-0.04}$	-	-

Table 2. The values of dark energy related quantities from the observations of baryon acoustic oscillation, RSD, SZ and lensing. In the second and third column “Planck” means “Planck TT,TE,EE+lowE+lensing”.

its equation of state. The linear growth factor of the dark matter density perturbations can be written as [54,55,56]

$$G(z) = 5 \frac{\Omega_m E(z)}{2} \int_z^\infty \frac{(1+z) dz}{E(z')^3} \quad (13)$$

where $E(z) = H(z)/H_0$ and $E(z)$ contains the by dark matter density (Ω_m) and dark energy density (Ω_Λ). The $5/2$ factor in the above equation is a normalization factor to make G equals to one at $a = 1$. In the case of the matter dominated Universe, the $G(z)$ becomes equal to $(1/1+z)$ or a . However, in the case of dark energy dominated Universe the situation changes and the growth factor is often denoted by a quantity

$$f = \frac{d \ln G}{d \ln a}. \quad (14)$$

Therefore, the deviation of f from the value of one provides the information about dark energy. It is customary to fit the $G(z)$ numerically and express it in terms of a monomial function of dark matter density fraction $\Omega_m(z)$ as

$$G(z) = \Omega_m(z)^\alpha. \quad (15)$$

The reason behind it is it makes the calculation of higher order perturbation analytically possible.

4.1 Redshift space distortion

Redshift space distortion imprints unique patterns on the distribution of the tracer field (galaxy or atomic hydrogen) which changes the position of the tracer field in redshift space depending on their peculiar velocities. Within the fully virialized objects, like the large halos, the peculiar velocities of the galaxies are much higher and random. However, on the larger scales the peculiar velocities are correlated to the density contrast and their magnitude can be predicted using the growth function in the ambit of cosmological perturbation theory. Therefore, the redshift space distortion provides an independent measurement of the growth factor along with the amplitude of the power spectrum.

In the redshift space, the power-spectrum loses its isotropic nature and its value depends on the direction of \mathbf{k} -vector with respect to the line of sight. In first order perturbation theory under plane parallel assumption the redshift space power spectrum can be written as

$$P_g^s(k, \mu) = b_1^2(1 + \beta\mu^2)^2 P(k), \quad (16)$$

where μ is the cosine of the angle between the \mathbf{k} -vector and the line of sight. To quantify this distortion it is customary to decompose the anisotropy in terms of spherical harmonics. In that case the monopole of the redshift space power-spectrum is amplified by the Kaiser factor which can be written as [57]

$$P_g^0(k) = b_1^2 \left(1 + \frac{2}{3}\beta + \frac{1}{5}\beta^2 \right) P(k). \quad (17)$$

Here, $\beta = f/b_1$. Similarly, the quadrupole and hexadecapoles can also be calculated. However, the model power-spectrum considered by BOSS-DR12 is even more complicated which contains not only the extension of the Kaiser model but also the higher order terms [58],

$$P_g^s(k, \mu) = \exp[-(fk\mu\sigma_v)^2] \{ P_{g,\delta\delta}(k) + 2f\mu^2 P_{g,\delta\theta}(k) + f^2\mu^4 P_{g,\delta\theta}(k) + \text{other correction terms} \}. \quad (18)$$

The exponential term defines the ‘‘Finger of God’’ effect due to the random velocities of the galaxies on the small scales. Here, θ is the divergence of the velocity fields of the galaxies, σ_v is the standard deviation of the velocity distribution of galaxies. Measurement of the multipoles of this power spectrum provides the value of $f(z)\sigma_8(z)$. For example the latest BOSS result provides the value of $f\sigma_8 = 0.289_{-0.096}^{+0.085}$ for $z_{\text{eff}} = 0.85$ [59]. Therefore, if σ_8 is measured from other complementary observation, then RSD can constrain the growth quite effectively. So, when Planck CMB data alone cannot constrain dark energy parameters effectively, RSD is incorporated in the analysis which provide the value of w_a and w_0 with reasonable accuracy (see table 2). In an earlier analysis of **BOSS-DR 11** power spectrum along with Planck provided the value of CPL parameters [60] to be $w_0 = -0.87_{-16}^{+15}$ and $w_a = -0.61_{0.61}^{+0.76}$.

However, the degeneracy between σ_8 and f cannot be broken with the observation of the redshift space power spectrum alone. For that purpose, it is essential to measure the bi-spectrum in the redshift space. The multipole moments of redshift space bi-spectrum for the second order perturbation theory has been studied in ref [61,62]. However, there do not exist any constraints on dark energy parameters using redshift space bispectrum as of now.

4.2 Lensing surveys

These surveys observe the lensing features, mainly the B-modes, produced by the large scale structures on CMB and traces back the lensing potential(ϕ) from that. The power spectrum of lensing potential ($C_\ell^{\phi\phi}$) can be theoretically obtained from the power-spectrum of the gravitational potentials (P_Ψ) [63,64].

$$C_\ell^{\phi\phi} = \frac{8\pi^2}{\ell^3} \int_0^{z_{\text{rec}}} \frac{dz}{H(z)} \chi(z) \left(\frac{\chi(z_{\text{rec}}) - \chi(z)}{\chi(z_{\text{rec}})\chi(z)} \right)^2 P_\Psi(z, k = \ell/\chi(z)) \quad (19)$$

Here $\chi(z)$ is the comoving distance at z . The power spectrum for gravitational potential is related to the matter power spectrum through the Poisson’s equation as

$$P_\Psi(z, k) = \frac{9\Omega_m(z)^2 H(z)^4}{8\pi^2} \frac{P(z, k)}{k} \quad (20)$$

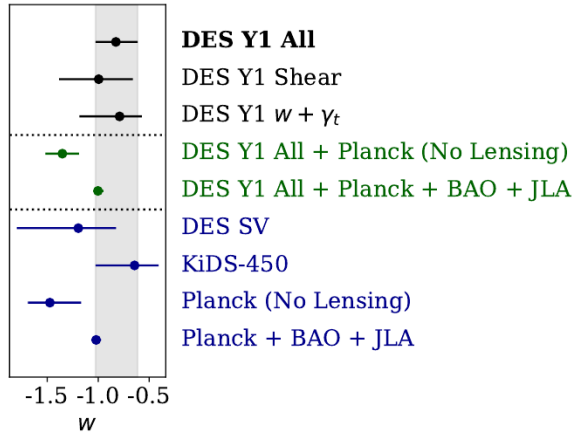


Fig. 3. Best-fit values of w for w CDM model from the lensing surveys (figure taken from ref [69]).

The non-linear matter power-spectrum is calculated using the `HaloFit` [65] extrapolation and linear matter power-spectrum as the input. The dependence of the linear matter spectrum on the growth function is discussed in the last subsection. Therefore, the dependence of the lensing potential with the growth factor is evident. The most important lensing surveys are CFHTLenS [53,66], KiDs [67], Planck Lensing survey [68] and DES [69]. The constraints on the equation of state in w CDM model from all the lensing surveys are shown in Fig. 3. The values of dark energy parameters constrained using lensing surveys are listed in table 2.

4.3 Sunyaev Zeldovich surveys

These surveys aim at counting the number of galaxy clusters from their SZ effect on CMB. In SZ effect [70,71,72] the black-body spectrum of the CMB gets distorted due to the inverse Compton scattering of CMB photon by the free electrons present in the intergalactic medium of the halo containing a galaxy cluster. Among the two types of SZ distortion known as μ distortion and y distortion, it is the y distortion that is mainly used to count the number of the clusters in the CMB surveys like space based Planck and ground based SPT and ACT survey. The masses of the observed clusters in SZ survey are assigned from the lensing survey. In this way, SZ surveys provide the number of halos in a given mass range and redshift range in the Universe. Theoretically the number density of halos of a given mass range can be calculated from the halo mass function. Although the simplest form of halo mass function, known as the Press-Schechter mass function can be calculated analytically, more accurate halo mass function requires N -body simulation. The most popular numerically fitted halo mass function is the Tinker [73] halo mass function which considers dark energy as cosmological constant. Whether different dark energy models will change the halo mass function or not is still an unresolved matter in cosmology. In general, it is assumed that halo mass function should depend on Ω_m and σ_8 only, which is known as the universality of halo mass function. However, it has been reported that different models of dark energy break the universality [74]. Recently it has been again claimed that universality can be restored by rescaling some variable [75]. Therefore, SZ surveys provide mainly the values of Ω_m and σ_8 and it cannot distinguish between the different dark energy models in an efficient way. However, when the measurements of σ_8 and Ω_m

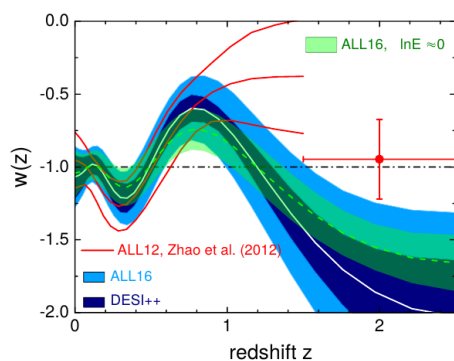


Fig. 4. Reconstruction of $w(z)$ from different data sets (11 BAO data sets and CFHTLens) shows that a dark energy behaves as a phantom field for significant range of redshift. The figure is taken from ref [79].

from an SZ survey is combined with other experiments it can provide reasonably good constraints on dark energy parameters. Planck SZ and BAO joint analysis provides $w = -1.01 \pm 0.18$ for w CDM model [76]. A recent joint analysis of DES and SPT has provided $w = -1.76^{+0.33}_{-0.46}$ for w CDM model along with varying neutrino mass [77].

5 Reconstruction of dark-energy equation of state from observations:

From the above discussions, we find that the most accurate determination of dark energy parameters come from the BAO and the measurement of the expansion of the Universe through the standard candles. Different galaxy surveys can provide BAO scales at different z values. As well as CMB can provide the estimation of angular scale at z_{rec} . Therefore, in recent years there has been series of attempts to reconstruct the $H(z)$ from the BAO values of different observations. The reconstruction of $H(z)$ also provides the reconstruction of the dark energy equation of state ($w(z)$) [78,79,80,81]. The reconstruction depends highly on the parametrization of the $w(z)$. However, there is a common finding among most of the studies. For some values of z , $w(z)$ becomes less than -1 . Any field which has an equation of state less than -1 is called the phantom field and therefore this type of dark energy is known as phantom dark energy. Some studies even show an oscillating feature in the dark energy equation of state (see Fig. 4).

6 H_0 tension and Dark energy:

The value of Hubble parameter inferred from the CMB and BAO measurements using the Λ CDM cosmology strongly disagrees with the Hubble value obtained from the direct measurement of HST [82]. This tension has opened up many possibilities of modifying the dark energy sector to resolve this tension. An incomplete list of such models includes early dark energy [83,84,85,86], interacting dark energy [87], dynamical dark energy [88] etc. However, it has been also argued that no model can resolve the H_0 tension by just modifying the dark energy dynamics in late time [89]. Here, we briefly review some of the features these models

- **Early dark energy** This solution proposes that some component of dark energy in the early times ($z \geq 3000$) behaves as a cosmological constant and makes a significant contribution to the energy density of the Universe. Then it decays down to radiation or some other component. This kind of models essentially modifies the growth rate of perturbations in the early times by modifying the background expansion rate for a certain period. However, there remain some issues with the early dark energy as it eases the tension between CMB and direct measurement of Hubble value but cannot resolve the tension between the inferred values from galaxy surveys and direct observation [90,91]. To resolve these issues further “new early dark energy” models are also proposed [92,93].
- **Interacting dark energy** In these models interaction between dark matter and dark energy are considered where the energy exchange is proportional to the four-velocity of the dark matter [94,95,96]. These models ease the tension between Planck and HST data. However, these models fail to resolve the tension between the BAO data and HST data [97].
- **Dynamical dark energy** As discussed earlier these types of model consider the dark energy equation of state to vary with time and CPL parameterization is the most popular way to of quantifying that variation. It has been shown that a joint analysis of Planck+HST data provides [88] $w_0 = -1.39^{+0.39}_{-0.32}$ and $w_a = -0.2^{+0.8}_{-1.6}$ and H_0 to be 73.9 ± 2.0 . However, when BAO+Planck data are considered the analysis provides a very low value of H_0 . Therefore, it cannot be claimed as a solution to the H_0 tension.

In spite of all these attempts, the very essence of H_0 tension is still intact. No other cosmological model except Λ CDM can fit the Planck CMB data alone with a better chi-squared value. The tension in between the different data-sets are still there and any solution which reduces the tension in H_0 increases the tension in σ_8 or other parameters.

7 σ_8 tension and Dark energy:

Moreover, it has also been reported that there is a mismatch between the value of σ_8 , the r.m.s fluctuations of density fluctuations at $8 h^{-1}\text{Mpc}^{-1}$, inferred from CMB fitted parameters under the Λ CDM framework and LSS observations [98,99,100]. This is commonly known as σ_8 tension. There have been a few attempts to resolve this tension by modifying the dark energy physics which includes interacting dark energy, dynamical dark energy etc [101,102,103,104,105,106,97,107,108,109]. In refs.[97,107], interaction between the dark energy and dark dark matter have been explored and they show that σ_8 tension significantly reduces in such models. In ref. [108], minimally and non-minimally coupled scalar field, which can act as the possible alternatives for dark energy, have been proposed to ease the σ_8 tension. In ref. [106], dynamical dark energy (CPL parameterization [4,5]) and $f(R)$ gravity model for dark energy have been analyzed and they find that σ_8 tension slightly decreases in the case of dynamical dark energy, whereas it worsens in case of $f(R)$ gravity model for dark energy. Furthermore, there are a few works that explore the running vacuum models as a resolution to the σ_8 tension [104,105]. The interested reader can see ref. [100] for a brief review on the current status of σ_8 tension.

8 Summary

In this article, we have briefly reviewed the methods and the current status of measuring dark energy parameters from different observations. The best measurement comes

from the baryon acoustic oscillation scales of Planck CMB data. For the case of the Λ CDM model experiments like the recent lensing observations (DES) or Planck data can provide significantly tight constraint by themselves. However, for the case of the w CDM model or dynamically varying dark energy models still, no single observation can constrain the parameters. In these cases, the joint analyses help to resolve the degeneracy between the parameters. For example, the RSD data of BOSS-DR12 can provide only the $f\sigma_8$ combination in a particular z_{eff} . SZ observations can provide a contour in the Ω_m - σ_8 plane. Lensing observations also provide the best constraints on the Ω_m - σ_8 plane. BAO from the galaxy surveys or Planck shows huge degeneracy in CPL parameters when analysed alone. But When Planck data is combined with RSD and lensing data it narrows down w_0 to -1 and w_a to 0 .

Different observations, although helps to break the degeneracy in the more complicated models, create tensions for the simplest models. The BAO data at different z values from different observations does not favor simple Λ CDM cosmology. Rather the recent reconstruction of the dark energy equation of state from these data sets has shown some hint of phantom dark energy for some particular ranges of redshift values. Similarly, the Hubble tension between the CMB and the direct detection of H_0 also opened up the scope of exploring different dark energy models.

References

1. S. Weinberg, *The Cosmological Constant Problem*, *Rev. Mod. Phys.* **61** (1989) 1–23.
2. **Supernova Search Team** Collaboration, A. G. Riess et al., *Observational evidence from supernovae for an accelerating universe and a cosmological constant*, *Astron. J.* **116** (1998) 1009–1038, [[astro-ph/9805201](#)].
3. **Supernova Cosmology Project** Collaboration, S. Perlmutter et al., *Measurements of Ω and Λ from 42 high redshift supernovae*, *Astrophys. J.* **517** (1999) 565–586, [[astro-ph/9812133](#)].
4. M. Chevallier and D. Polarski, *Accelerating universes with scaling dark matter*, *Int. J. Mod. Phys. D* **10** (2001) 213–224, [[gr-qc/0009008](#)].
5. E. V. Linder, *Exploring the expansion history of the universe*, *Phys. Rev. Lett.* **90** (2003) 091301, [[astro-ph/0208512](#)].
6. S. PERLMUTTER, *Supernovae, dark energy, and the accelerating universe: The status of the cosmological parameters*, *International Journal of Modern Physics A* **15** (2000), no. supp01b 715–739, [<https://doi.org/10.1142/S0217751X00005383>].
7. D. M. Scolnic et al., *The Complete Light-curve Sample of Spectroscopically Confirmed SNe Ia from Pan-STARRS1 and Cosmological Constraints from the Combined Pantheon Sample*, *Astrophys. J.* **859** (2018), no. 2 101, [[arXiv:1710.00845](#)].
8. **DES** Collaboration, T. M. C. Abbott et al., *First Cosmology Results using Type Ia Supernovae from the Dark Energy Survey: Constraints on Cosmological Parameters*, *Astrophys. J. Lett.* **872** (2019), no. 2 L30, [[arXiv:1811.02374](#)].
9. **Planck** Collaboration, P. A. R. Ade et al., *Planck 2015 results. XIII. Cosmological parameters*, *Astron. Astrophys.* **594** (2016) A13, [[arXiv:1502.01589](#)].
10. F. Beutler, C. Blake, M. Colless, D. H. Jones, L. Staveley-Smith, L. Campbell, Q. Parker, W. Saunders, and F. Watson, *The 6dF Galaxy Survey: Baryon Acoustic Oscillations and the Local Hubble Constant*, *Mon. Not. Roy. Astron. Soc.* **416** (2011) 3017–3032, [[arXiv:1106.3366](#)].
11. **BOSS** Collaboration, L. Anderson et al., *The clustering of galaxies in the SDSS-III Baryon Oscillation Spectroscopic Survey: baryon acoustic oscillations in the Data Releases 10 and 11 Galaxy samples*, *Mon. Not. Roy. Astron. Soc.* **441** (2014), no. 1 24–62, [[arXiv:1312.4877](#)].
12. A. J. Ross, L. Samushia, C. Howlett, W. J. Percival, A. Burden, and M. Manera, *The clustering of the SDSS DR7 main Galaxy sample – I. A 4 per cent distance measure at $z = 0.15$* , *Mon. Not. Roy. Astron. Soc.* **449** (2015), no. 1 835–847, [[arXiv:1409.3242](#)].

13. **BOSS** Collaboration, S. Alam et al., *The clustering of galaxies in the completed SDSS-III Baryon Oscillation Spectroscopic Survey: cosmological analysis of the DR12 galaxy sample*, *Mon. Not. Roy. Astron. Soc.* **470** (2017), no. 3 2617–2652, [[arXiv:1607.03155](#)].
14. A. G. Riess et al., *BV RI light curves for 22 type Ia supernovae*, *Astron. J.* **117** (1999) 707–724, [[astro-ph/9810291](#)].
15. S. Jha et al., *Uvri light curves of 44 type ia supernovae*, *Astron. J.* **131** (2006) 527–554, [[astro-ph/0509234](#)].
16. M. Hicken, W. M. Wood-Vasey, S. Blondin, P. Challis, S. Jha, P. L. Kelly, A. Rest, and R. P. Kirshner, *Improved Dark Energy Constraints from ~100 New CfA Supernova Type Ia Light Curves*, *Astrophys. J.* **700** (2009) 1097–1140, [[arXiv:0901.4804](#)].
17. M. Hicken, P. Challis, S. Jha, R. P. Kirshner, T. Matheson, M. Modjaz, A. Rest, and W. M. Wood-Vasey, *CfA3: 185 Type Ia Supernova Light Curves from the CfA*, *Astrophys. J.* **700** (2009) 331–357, [[arXiv:0901.4787](#)].
18. M. Hicken et al., *CfA4: Light Curves for 94 Type Ia Supernovae*, *Astrophys. J. Suppl.* **200** (2012) 12, [[arXiv:1205.4493](#)].
19. C. Contreras et al., *The Carnegie Supernova Project: First Photometry Data Release of Low-Redshift Type Ia Supernovae*, *Astron. J.* **139** (2010) 519–539, [[arXiv:0910.3330](#)].
20. G. Folatelli et al., *The Carnegie Supernova Project: Analysis of the First Sample of Low-Redshift Type-Ia Supernovae*, *Astron. J.* **139** (2010) 120–144, [[arXiv:0910.3317](#)].
21. M. D. Stritzinger et al., *The Carnegie Supernova Project: Second Photometry Data Release of Low-Redshift Type Ia Supernovae*, *Astron. J.* **142** (2011) 156, [[arXiv:1108.3108](#)].
22. M. Ganeshalingam, W. Li, and A. V. Filippenko, *Constraints on dark energy with the LOSS SN Ia sample*, *Mon. Not. Roy. Astron. Soc.* **433** (2013) 2240, [[arXiv:1307.0824](#)].
23. G. Miknaitis et al., *The ESSENCE Supernova Survey: Survey Optimization, Observations, and Supernova Photometry*, *Astrophys. J.* **666** (2007) 674–693, [[astro-ph/0701043](#)].
24. **ESSENCE** Collaboration, W. M. Wood-Vasey et al., *Observational Constraints on the Nature of the Dark Energy: First Cosmological Results from the ESSENCE Supernova Survey*, *Astrophys. J.* **666** (2007) 694–715, [[astro-ph/0701041](#)].
25. G. Narayan et al., *Light Curves of 213 Type Ia Supernovae from the ESSENCE Survey*, *Astrophys. J. Suppl.* **224** (2016), no. 1 3, [[arXiv:1603.03823](#)].
26. **SNLS** Collaboration, A. Conley et al., *Supernova Constraints and Systematic Uncertainties from the First 3 Years of the Supernova Legacy Survey*, *Astrophys. J. Suppl.* **192** (2011) 1, [[arXiv:1104.1443](#)].
27. **SNLS** Collaboration, M. Sullivan et al., *SNLS3: Constraints on Dark Energy Combining the Supernova Legacy Survey Three Year Data with Other Probes*, *Astrophys. J.* **737** (2011) 102, [[arXiv:1104.1444](#)].
28. J. A. Frieman et al., *The Sloan Digital Sky Survey-II Supernova Survey: Technical Summary*, *Astron. J.* **135** (2008) 338–347, [[arXiv:0708.2749](#)].
29. R. Kessler et al., *First-year Sloan Digital Sky Survey-II (SDSS-II) Supernova Results: Hubble Diagram and Cosmological Parameters*, *Astrophys. J. Suppl.* **185** (2009) 32–84, [[arXiv:0908.4274](#)].
30. **SDSS** Collaboration, M. Sako et al., *The Data Release of the Sloan Digital Sky Survey-II Supernova Survey*, *Publ. Astron. Soc. Pac.* **130** (2018), no. 988 064002, [[arXiv:1401.3317](#)].
31. A. Rest et al., *Cosmological Constraints from Measurements of Type Ia Supernovae discovered during the first 1.5 yr of the Pan-STARRS1 Survey*, *Astrophys. J.* **795** (2014), no. 1 44, [[arXiv:1310.3828](#)].
32. D. Scolnic et al., *Systematic Uncertainties Associated with the Cosmological Analysis of the First Pan-STARRS1 Type Ia Supernova Sample*, *Astrophys. J.* **795** (2014), no. 1 45, [[arXiv:1310.3824](#)].

33. **Supernova Cosmology Project** Collaboration, N. Suzuki et al., *The Hubble Space Telescope Cluster Supernova Survey: V. Improving the Dark Energy Constraints Above $z > 1$ and Building an Early-Type-Hosted Supernova Sample*, *Astrophys. J.* **746** (2012) 85, [arXiv:1105.3470].
34. **Supernova Search Team** Collaboration, A. G. Riess et al., *Type Ia supernova discoveries at $z > 1$ from the Hubble Space Telescope: Evidence for past deceleration and constraints on dark energy evolution*, *Astrophys. J.* **607** (2004) 665–687, [astro-ph/0402512].
35. A. G. Riess et al., *New Hubble Space Telescope Discoveries of Type Ia Supernovae at $z \geq 1$: Narrowing Constraints on the Early Behavior of Dark Energy*, *Astrophys. J.* **659** (2007) 98–121, [astro-ph/0611572].
36. O. Graur et al., *Type-Ia Supernova Rates to Redshift 2.4 from CLASH: the Cluster Lensing And Supernova survey with Hubble*, *Astrophys. J.* **783** (2014) 28, [arXiv:1310.3495].
37. S. A. Rodney et al., *Type Ia Supernova Rate Measurements to Redshift 2.5 from CANDELS : Searching for Prompt Explosions in the Early Universe*, *Astron. J.* **148** (2014) 13, [arXiv:1401.7978].
38. A. G. Riess et al., *Type Ia Supernova Distances at Redshift > 1.5 from the Hubble Space Telescope Multi-cycle Treasury Programs: The Early Expansion Rate*, *Astrophys. J.* **853** (2018), no. 2 126, [arXiv:1710.00844].
39. J. Colin, R. Mohayaee, M. Rameez, and S. Sarkar, *Evidence for anisotropy of cosmic acceleration*, *Astron. Astrophys.* **631** (2019) L13, [arXiv:1808.04597].
40. D. J. Eisenstein and M. J. White, *Theoretical uncertainty in baryon oscillations*, *Phys. Rev. D* **70** (2004) 103523, [astro-ph/0407539].
41. B. A. Bassett and R. Hlozek, *Baryon Acoustic Oscillations*, arXiv:0910.5224.
42. **Planck** Collaboration, N. Aghanim et al., *Planck 2018 results. VI. Cosmological parameters*, *Astron. Astrophys.* **641** (2020) A6, [arXiv:1807.06209].
43. C.-P. Ma and E. Bertschinger, *Cosmological perturbation theory in the synchronous and conformal Newtonian gauges*, *Astrophys. J.* **455** (1995) 7–25, [astro-ph/9506072].
44. **ACT** Collaboration, S. Aiola et al., *The Atacama Cosmology Telescope: DR4 Maps and Cosmological Parameters*, *JCAP* **12** (2020) 047, [arXiv:2007.07288].
45. **SPT** Collaboration, L. Balkenhol et al., *Constraints on Λ CDM Extensions from the SPT-3G 2018 EE and TE Power Spectra*, arXiv:2103.13618.
46. L. Anderson et al., *The clustering of galaxies in the SDSS-III Baryon Oscillation Spectroscopic Survey: Baryon Acoustic Oscillations in the Data Release 9 Spectroscopic Galaxy Sample*, *Mon. Not. Roy. Astron. Soc.* **427** (2013), no. 4 3435–3467, [arXiv:1203.6594].
47. **2dFGRS** Collaboration, S. Cole et al., *The 2dF Galaxy Redshift Survey: Power-spectrum analysis of the final dataset and cosmological implications*, *Mon. Not. Roy. Astron. Soc.* **362** (2005) 505–534, [astro-ph/0501174].
48. **SDSS** Collaboration, W. J. Percival et al., *Baryon Acoustic Oscillations in the Sloan Digital Sky Survey Data Release 7 Galaxy Sample*, *Mon. Not. Roy. Astron. Soc.* **401** (2010) 2148–2168, [arXiv:0907.1660].
49. C. Blake et al., *The WiggleZ Dark Energy Survey: mapping the distance-redshift relation with baryon acoustic oscillations*, *Mon. Not. Roy. Astron. Soc.* **418** (2011) 1707–1724, [arXiv:1108.2635].
50. R. Laureijs and et.al, *Euclid Definition Study Report*, arXiv e-prints (Oct., 2011) arXiv:1110.3193, [arXiv:1110.3193].
51. **DESI** Collaboration, M. Levi et al., *The DESI Experiment, a whitepaper for Snowmass 2013*, arXiv:1308.0847 (8, 2013).
52. **BOSS** Collaboration, G.-B. Zhao et al., *The clustering of galaxies in the completed SDSS-III Baryon Oscillation Spectroscopic Survey: tomographic BAO analysis of DR12 combined sample in Fourier space*, *Mon. Not. Roy. Astron. Soc.* **466** (2017), no. 1 762–779, [arXiv:1607.03153].

53. C. Heymans et al., *CFHTLenS tomographic weak lensing cosmological parameter constraints: Mitigating the impact of intrinsic galaxy alignments*, *Mon. Not. Roy. Astron. Soc.* **432** (2013) 2433, [[arXiv:1303.1808](#)].
54. D. J. Heath, *The growth of density perturbations in zero pressure Friedmann-Lemaître universes.*, *Mon. Not. Roy. Astron. Soc.* **179** (May, 1977) 351–358.
55. D. J. Eisenstein, *An Analytic expression for the growth function in a flat universe with a cosmological constant*, [astro-ph/9709054](#).
56. A. J. S. Hamilton, *Formulae for growth factors in expanding universes containing matter and a cosmological constant*, *Mon. Not. Roy. Astron. Soc.* **322** (2001) 419, [[astro-ph/0006089](#)].
57. N. Kaiser, *Clustering in real space and in redshift space*, *Mon. Not. Roy. Astron. Soc.* **227** (1987) 1–27.
58. **BOSS** Collaboration, F. Beutler et al., *The clustering of galaxies in the completed SDSS-III Baryon Oscillation Spectroscopic Survey: Anisotropic galaxy clustering in Fourier-space*, *Mon. Not. Roy. Astron. Soc.* **466** (2017), no. 2 2242–2260, [[arXiv:1607.03150](#)].
59. A. de Mattia et al., *The Completed SDSS-IV extended Baryon Oscillation Spectroscopic Survey: measurement of the BAO and growth rate of structure of the emission line galaxy sample from the anisotropic power spectrum between redshift 0.6 and 1.1*, [arXiv:2007.09008](#).
60. A. Upadhye, *Neutrino mass and dark energy constraints from redshift-space distortions*, *JCAP* **05** (2019) 041, [[arXiv:1707.09354](#)].
61. R. Scoccimarro, H. M. P. Couchman, and J. A. Frieman, *The Bispectrum as a Signature of Gravitational Instability in Redshift-Space*, *Astrophys. J.* **517** (1999) 531–540, [[astro-ph/9808305](#)].
62. A. Mazumdar, S. Bharadwaj, and D. Sarkar, *Quantifying the Redshift Space Distortion of the Bispectrum II: Induced Non-Gaussianity at Second Order Perturbation*, *Mon. Not. Roy. Astron. Soc.* **498** (2020), no. 3 3975–3984, [[arXiv:2005.07066](#)].
63. A. Lewis and A. Challinor, *Weak gravitational lensing of the CMB*, *Phys. Rept.* **429** (2006) 1–65, [[astro-ph/0601594](#)].
64. K. M. Smith et al., *CMBPol Mission Concept Study: Gravitational Lensing*, *AIP Conf. Proc.* **1141** (2009), no. 1 121, [[arXiv:0811.3916](#)].
65. **VIRGO Consortium** Collaboration, R. E. Smith, J. A. Peacock, A. Jenkins, S. D. M. White, C. S. Frenk, F. R. Pearce, P. A. Thomas, G. Efstathiou, and H. M. P. Couchmann, *Stable clustering, the halo model and nonlinear cosmological power spectra*, *Mon. Not. Roy. Astron. Soc.* **341** (2003) 1311, [[astro-ph/0207664](#)].
66. T. Erben et al., *CFHTLenS: The Canada-France-Hawaii Telescope Lensing Survey - Imaging Data and Catalogue Products*, *Mon. Not. Roy. Astron. Soc.* **433** (2013) 2545, [[arXiv:1210.8156](#)].
67. H. Hildebrandt et al., *KiDS-450: Cosmological parameter constraints from tomographic weak gravitational lensing*, *Mon. Not. Roy. Astron. Soc.* **465** (2017) 1454, [[arXiv:1606.05338](#)].
68. **Planck** Collaboration, N. Aghanim et al., *Planck 2018 results. VIII. Gravitational lensing*, *Astron. Astrophys.* **641** (2020) A8, [[arXiv:1807.06210](#)].
69. **DES** Collaboration, T. M. C. Abbott et al., *Dark Energy Survey year 1 results: Cosmological constraints from galaxy clustering and weak lensing*, *Phys. Rev. D* **98** (2018), no. 4 043526, [[arXiv:1708.01530](#)].
70. R. A. Sunyaev and Y. B. Zeldovich, *Small scale fluctuations of relic radiation*, *Astrophys. Space Sci.* **7** (1970) 3–19.
71. R. A. Sunyaev and Y. B. Zeldovich, *The Observations of relic radiation as a test of the nature of X-Ray radiation from the clusters of galaxies*, *Comments Astrophys. Space Phys.* **4** (1972) 173–178.
72. R. A. Sunyaev and Y. B. Zeldovich, *Microwave background radiation as a probe of the contemporary structure and history of the universe*, *Ann. Rev. Astron. Astrophys.* **18** (1980) 537–560.

73. J. L. Tinker, A. V. Kravtsov, A. Klypin, K. Abazajian, M. S. Warren, G. Yepes, S. Gottlober, and D. E. Holz, *Toward a halo mass function for precision cosmology: The Limits of universality*, *Astrophys. J.* **688** (2008) 709–728, [[arXiv:0803.2706](#)].
74. J. Courtin, Y. Rasera, J. M. Alimi, P. S. Corasaniti, V. Boucher, and A. Fuzfa, *Imprints of dark energy on cosmic structure formation: II) Non-Universality of the halo mass function*, *Mon. Not. Roy. Astron. Soc.* **410** (2011) 1911–1931, [[arXiv:1001.3425](#)].
75. G. Despali, C. Giocoli, R. E. Angulo, G. Tormen, R. K. Sheth, G. Baso, and L. Moscardini, *The universality of the virial halo mass function and models for non-universality of other halo definitions*, *Mon. Not. Roy. Astron. Soc.* **456** (2016), no. 3 2486–2504, [[arXiv:1507.05627](#)].
76. **Planck** Collaboration, P. A. R. Ade et al., *Planck 2015 results. XXIV. Cosmology from Sunyaev-Zeldovich cluster counts*, *Astron. Astrophys.* **594** (2016) A24, [[arXiv:1502.01597](#)].
77. **DES, SPT** Collaboration, M. Costanzi et al., *Cosmological constraints from DES Y1 cluster abundances and SPT multiwavelength data*, *Phys. Rev. D* **103** (2021), no. 4 043522, [[arXiv:2010.13800](#)].
78. G.-B. Zhao, R. G. Crittenden, L. Pogosian, and X. Zhang, *Examining the evidence for dynamical dark energy*, *Phys. Rev. Lett.* **109** (2012) 171301, [[arXiv:1207.3804](#)].
79. G.-B. Zhao et al., *Dynamical dark energy in light of the latest observations*, *Nature Astron.* **1** (2017), no. 9 627–632, [[arXiv:1701.08165](#)].
80. J.-P. Dai, Y. Yang, and J.-Q. Xia, *Reconstruction of the Dark Energy Equation of State from the Latest Observations*, *Astrophys. J.* **857** (2018), no. 1 9.
81. B. R. Dinda, *Model independent parametrization of the late time cosmic acceleration: Constraints on the parameters from recent observations*, *Phys. Rev. D* **100** (2019), no. 4 043528, [[arXiv:1904.10418](#)].
82. G. Efstathiou, *H0 Revisited*, *Mon. Not. Roy. Astron. Soc.* **440** (2014), no. 2 1138–1152, [[arXiv:1311.3461](#)].
83. T. Karwal and M. Kamionkowski, *Dark energy at early times, the Hubble parameter, and the string axiverse*, *Phys. Rev. D* **94** (2016), no. 10 103523, [[arXiv:1608.01309](#)].
84. V. Poulin, T. L. Smith, D. Grin, T. Karwal, and M. Kamionkowski, *Cosmological implications of ultralight axionlike fields*, *Phys. Rev. D* **98** (2018), no. 8 083525, [[arXiv:1806.10608](#)].
85. V. Poulin, T. L. Smith, T. Karwal, and M. Kamionkowski, *Early Dark Energy Can Resolve The Hubble Tension*, *Phys. Rev. Lett.* **122** (2019), no. 22 221301, [[arXiv:1811.04083](#)].
86. T. L. Smith, V. Poulin, and M. A. Amin, *Oscillating scalar fields and the Hubble tension: a resolution with novel signatures*, *Phys. Rev. D* **101** (2020), no. 6 063523, [[arXiv:1908.06995](#)].
87. E. Di Valentino, A. Melchiorri, and O. Mena, *Can interacting dark energy solve the H₀ tension?*, *Phys. Rev. D* **96** (2017), no. 4 043503, [[arXiv:1704.08342](#)].
88. E. Di Valentino, A. Melchiorri, E. V. Linder, and J. Silk, *Constraining Dark Energy Dynamics in Extended Parameter Space*, *Phys. Rev. D* **96** (2017), no. 2 023523, [[arXiv:1704.00762](#)].
89. R.-Y. Guo, J.-F. Zhang, and X. Zhang, *Can the H₀ tension be resolved in extensions to Λ CDM cosmology?*, *JCAP* **02** (2019) 054, [[arXiv:1809.02340](#)].
90. J. C. Hill, E. McDonough, M. W. Toomey, and S. Alexander, *Early dark energy does not restore cosmological concordance*, *Phys. Rev. D* **102** (2020), no. 4 043507, [[arXiv:2003.07355](#)].
91. M. M. Ivanov, E. McDonough, J. C. Hill, M. Simonović, M. W. Toomey, S. Alexander, and M. Zaldarriaga, *Constraining Early Dark Energy with Large-Scale Structure*, *Phys. Rev. D* **102** (2020), no. 10 103502, [[arXiv:2006.11235](#)].
92. F. Niedermann and M. S. Sloth, *New Early Dark Energy is compatible with current LSS data*, [arXiv:2009.00006](#).
93. F. Niedermann and M. S. Sloth, *Resolving the Hubble Tension with New Early Dark Energy*, [arXiv:2006.06686](#).

94. J. Valiviita, E. Majerotto, and R. Maartens, *Instability in interacting dark energy and dark matter fluids*, *JCAP* **07** (2008) 020, [[arXiv:0804.0232](#)].
95. L. Vergani, L. P. L. Colombo, G. La Vacca, and S. A. Bonometto, *Dark Matter - Dark Energy coupling biasing parameter estimates from CMB data*, *Astrophys. J.* **697** (2009) 1946–1955, [[arXiv:0804.0285](#)].
96. L. Lopez Honorez, B. A. Reid, O. Mena, L. Verde, and R. Jimenez, *Coupled dark matter-dark energy in light of near Universe observations*, *JCAP* **09** (2010) 029, [[arXiv:1006.0877](#)].
97. E. Di Valentino, A. Melchiorri, O. Mena, and S. Vagnozzi, *Interacting dark energy in the early 2020s: A promising solution to the H_0 and cosmic shear tensions*, *Phys. Dark Univ.* **30** (2020) 100666, [[arXiv:1908.04281](#)].
98. S. Joudaki et al., *KiDS-450: Testing extensions to the standard cosmological model*, *Mon. Not. Roy. Astron. Soc.* **471** (2017), no. 2 1259–1279, [[arXiv:1610.04606](#)].
99. S. Mohanty, S. Anand, P. Chabul, A. Mazumdar, and P. Parashari, *σ_8 Discrepancy and its solutions*, *J. Astrophys. Astron.* **39** (2018), no. 4 46.
100. E. Di Valentino et al., *Cosmology Intertwined III: $f\sigma_8$ and S_8* , [arXiv:2008.11285](#).
101. A. Pourtsidou and T. Tram, *Reconciling CMB and structure growth measurements with dark energy interactions*, *Phys. Rev.* **D94** (2016), no. 4 043518, [[arXiv:1604.04222](#)].
102. V. Salvatelli, N. Said, M. Bruni, A. Melchiorri, and D. Wands, *Indications of a late-time interaction in the dark sector*, *Phys. Rev. Lett.* **113** (2014), no. 18 181301, [[arXiv:1406.7297](#)].
103. W. Yang and L. Xu, *Cosmological constraints on interacting dark energy with redshift-space distortion after Planck data*, *Phys. Rev.* **D89** (2014), no. 8 083517, [[arXiv:1401.1286](#)].
104. A. Gomez-Valent and J. Sola, *Relaxing the σ_8 -tension through running vacuum in the Universe*, *EPL* **120** (2017), no. 3 39001, [[arXiv:1711.00692](#)].
105. A. Gómez-Valent and J. Solà, *Density perturbations for running vacuum: a successful approach to structure formation and to the σ_8 -tension*, [arXiv:1801.08501](#).
106. G. Lambiase, S. Mohanty, A. Narang, and P. Parashari, *Testing dark energy models in the light of σ_8 tension*, *Eur. Phys. J. C* **79** (2019), no. 2 141, [[arXiv:1804.07154](#)].
107. E. Di Valentino, A. Melchiorri, O. Mena, and S. Vagnozzi, *Nonminimal dark sector physics and cosmological tensions*, *Phys. Rev. D* **101** (2020), no. 6 063502, [[arXiv:1910.09853](#)].
108. Z. Davari, V. Marra, and M. Malekjani, *Cosmological constraints on minimally and non-minimally coupled scalar field models*, *Mon. Not. Roy. Astron. Soc.* **491** (2020), no. 2 1920–1933, [[arXiv:1911.00209](#)].
109. P. Parashari, S. Anand, P. Chabul, G. Lambiase, S. Mohanty, A. Mazumdar, and A. Narang, *Status of σ_8 Tension in Different Cosmological Models*, *Springer Proc. Phys.* **261** (2021) 907–912.